

Dynamics of the refractive index induced in germanosilicate optical fibres by different types of UV irradiation

E M Dianov, S A Vasil'ev[¶], O I Medvedkov, A A Frolov

Abstract. A Mach–Zehnder fibre interferometer, based on two photoinduced long-period gratings, was used in an investigation of the dynamics of the refractive index Δn_{ind} induced in the core of a germanosilicate optical fibre by different types of UV irradiation. It was found that the value of Δn_{ind} could be approximated satisfactorily by a power-law function of the radiation dose at all the investigated wavelengths. A comparative analysis of the dynamics of the refractive index in the case of singlet and triplet photoexcitation of germanium oxygen-deficient centres showed that the dominant mechanism of the change in the refractive index by low-intensity continuous UV irradiation was transformation of these centres from an excited triplet state.

1. Introduction

In spite of the wide use of the photoinduced changes in the refractive index (RI) of germanosilicate fibres in fabrication of intracavity RI gratings [1], the nature and the microscopic mechanisms of the photosensitivity of glass are not yet fully understood. Several models have been put forward to explain the phenomena which occur during UV irradiation of optical fibres: transformation of defects in the glass network [2], relaxation of initial elastic stresses in the fibre core [3], and photoactivated densification of glass [4]. However, none of these models can ensure a full agreement with the experimental observations. On the other hand, there is no doubt that the main role, at least in the initial stages of the photoinduced transformations in germanosilicate fibres leading to changes in the RI, is played by germanium oxygen-deficient centres (GODCs). It is the strong absorption band with its maximum at $\lambda = 242$ nm, attributed to singlet–singlet absorption in GODCs, which is usually employed to form RI gratings in germanosilicate fibres.

We demonstrated earlier [5, 6] that photoexcitation to the singlet–triplet ($S_0 - T_1$) absorption band of GODCs with its maximum near 330 nm leads to processes similar to those

occurring in the singlet–singlet ($S_0 - S_1$) excitation. For example, marked decay of the triplet ($T_1 - S_0$) luminescence of the GODCs with its maximum near 400 nm is observed, paramagnetic E' germanium centres are formed, and the concentration of the luminescence centres with a maximum at $\lambda = 650$ nm (Ge-DID defects [3]) increases. Finally, we found that direct triplet photoexcitation induces an RI change sufficient for the formation of gratings in the core of a fibre [7]. A comparative analysis of long-period gratings formed by radiations with $\lambda = 333 - 364$ and 248 nm demonstrated that all these gratings are characterised by almost the same thermal stability.

These results led us to propose a hypothesis that in the microscopic mechanism of the induced RI changes the main role is played by a long-lived ($\tau \approx 100$ μs) excited triplet state of the GODCs [7]. One of the possible models of such a process was proposed in Ref. [8], where calculations were reported of the energy diagrams of GODCs and it was shown that only a small energy barrier (~ 0.2 eV) has to be overcome for a transition of a GODC from the T_1 state to an asymmetrically relaxed state. In this mechanism of the transformation of the GODCs by a fast ($\tau \sim 5.3$ ns at $T = 300$ K [9]) intercombination transition from the S_1 to T_1 state the excitation of S_1 plays solely the role of an effective channel for populating the T_1 state and even in the direct singlet photoexcitation this GODC transformation process is the dominant one.

In the investigation reported below we identified the contribution of this mechanism to the induced RI by a comparative analysis of the RI dynamics in the core of a germanosilicate fibre waveguide subjected to different types of photoexcitation at the wavelengths of the singlet and triplet absorption bands of GODCs.

2. Experiments

In our experiments we used a germanosilicate step-index fibre with $\Delta n \approx 0.02$, a cutoff wavelength of $\lambda_c = 1.04$ μm , and a cladding diameter of 125 μm . The dynamics of the photoinduced RI changes in the core were studied by an interferometric method, the principle of which was described in Ref. [10]. A Mach–Zehnder interferometer was inscribed in the investigated fibre: it was formed by two long-period RI gratings with the branching ratio 3 dB, coupling the fundamental and cladding modes of the fibre.

In the first grating, half the power of the fundamental waveguide mode was converted into the cladding mode. Half the power thus travelled the distance between the first and second gratings as the cladding mode and the other half as the fundamental mode. The modes interacted in the second grating in accordance with the phase difference $\Delta\phi$,

[¶]This author's name is sometimes spelt Vasiliev in the Western literature.

which they acquired travelling between the gratings. Consequently, the transmission spectrum of this interferometer was sensitive to $\Delta\phi$. Since the power of the cladding mode propagating along the core was low, the RI change in the core resulted mainly in a change in the propagation constant of the fundamental mode. Therefore, determination of the phase shift of the interference pattern, formed as a result of lateral UV irradiation of the region between the gratings, made it possible to determine the RI induced in the fibre core.

These long-period gratings were written by the 'point-by-point' method [7] employing cw radiation representing the second harmonic of an argon laser ($\lambda = 244$ nm) of power density ~ 15 kW cm $^{-2}$. The total dose was ~ 150 kJ cm $^{-2}$. The grating period was selected to be 200 μ m to ensure that the resonant coupling between the core and cladding modes employed in this experiment occurred in a spectral range convenient for the investigation. The lengths of the gratings forming the interferometer were ~ 7 mm and the separation between them was ~ 25 mm. The characteristic transmission spectrum of the interferometer, formed by interference of the HE_{11} and HE_{1n} ($n = 8, 9$) modes, is shown in Fig. 1. As demonstrated in Ref. [10], this interferometric scheme can ensure a high precision ($\sim 10^{-6}$) of measurement of the photoinduced RI in the fibre core, has a better temperature stability than the traditional interferometric methods [2], and does not require numerous assumptions about the grating parameters usually employed in the methods based on an analysis of the reflection spectra of Bragg gratings [11, 12, 13].

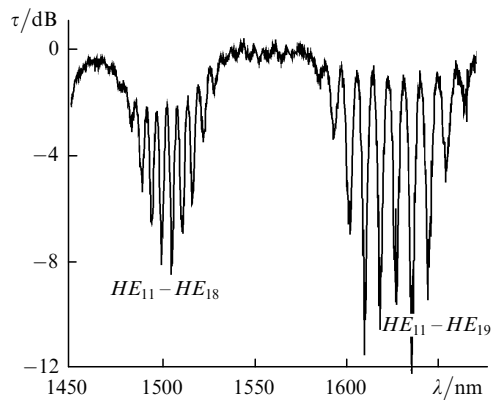


Figure 1. Transmission spectrum of a Mach-Zehnder interferometer.

The dynamics of the induced RI was studied by removing the protective cladding from a part of a fibre ($L \sim 5$ mm) located between gratings 1 and 2 and by exposing this bare part to UV radiation from various sources (Fig. 2a). Measurements were carried out employing three UV lasers: a pulsed excimer KrF laser ($\lambda = 248$ nm, $E_p \sim 100$ mJ, $\tau_p \sim 20$ ns), the second harmonic of a cw Ar $^+$ laser ($\lambda = 244$ nm, $P \sim 100$ mW), and an Ar $^+$ laser emitting simultaneously at several UV wavelengths ($\lambda = 333-364$ nm, $P \sim 500$ mW). The radiation from the last laser consisted of a set of spectral lines with the intensity ratio $I_{333} : I_{351} : I_{364} = 0.12 : 0.47 : 0.41$, which was independent of the total output power.

A beam-limiting aperture (Fig. 2a) selected the spatially uniform part of the beam and determined the length of the irradiated part L of the fibre. The power density of the radiation reaching the fibre surface was varied by altering the

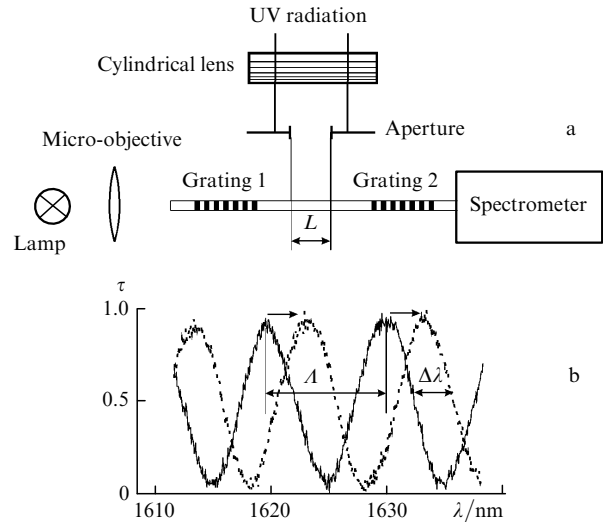


Figure 2. System used to study the dynamics of the RI changes induced in the core of a fibre waveguide (a) and the changes in the transmission spectrum of an interferometer as a result of UV irradiation (b).

distance between the fibre and a cylindrical lens ($f = 10$ cm). The transmission spectrum of the interferometer was recorded with a spectral resolution of 2 nm employing a tungsten halogen lamp and an optical spectrum analyser. The spectral shift $\Delta\lambda$ of the interference pattern (Fig. 2b) was recorded. This shift was related to the RI induced in the core Δn_{ind} by:

$$\Delta n_{\text{ind}} = \frac{\lambda \Delta\lambda}{L A \eta}, \quad (1)$$

where λ is the wavelength near which the measurements were carried out; A is the interference period; η is the fraction of the power of the fundamental mode propagating along the fibre core.

3. Results and discussion

Fig. 3 gives the dependences of the induced RI on the radiation dose D delivered by our sources. An analysis shows that all these dependences can be approximated satisfactorily by a straight line plotted on a double logarithmic scale, i.e. by power functions of the dose ($\Delta n_{\text{ind}} \propto D^b$) for all types of irradiation in wide ranges of the RI changes ($10^{-5} - 5 \times 10^{-4}$), of the radiation intensities, and of the doses ($5 \times 10^{-2} - 10^{-4}$ J cm $^{-2}$ for singlet irradiation). Similar laws governing the RI changes were reported elsewhere [12, 13], but an explanation of such dependences has not yet been proposed. The power exponent b is not constant: it depends on the type of radiation and its intensity. For example, pulsed and strong cw ($I_{244} > 1$ W cm $^{-2}$) irradiation is characterised by $b \approx 0.3 - 0.4$, in good agreement with the published results [12, 13], whereas for the low-intensity ($I_{244} < 1$ W cm $^{-2}$) singlet and triplet excitation the value of b increases to 0.5. It should also be pointed out that for $I_{244} < 1$ W cm $^{-2}$ the induced RI depends only on the total radiation dose, indicating that the process is of one-photon nature.

It is clear from Fig. 3 that pulsed radiation ($\lambda = 248$ nm) is at least an order more effective in inducing RI changes than continuous radiation ($\lambda = 244$ nm). One of the reasons for this difference could be thermally activated acceleration of the process of inducing the RI by heating of the irradiated

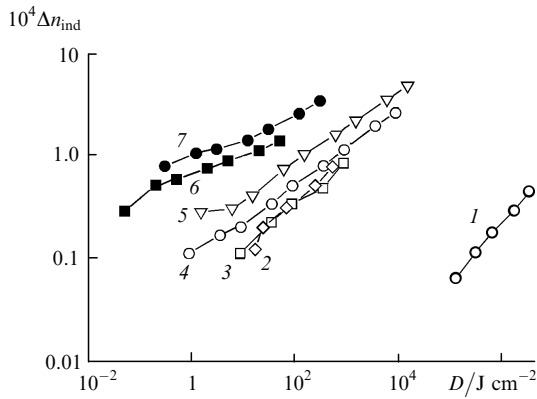


Figure 3. Dependences of the induced RI on the dose of cw $\lambda = 333\text{--}364$ nm radiation of 300 W cm^{-2} intensity (1) and of cw $\lambda = 244$ nm radiation of intensities 0.08 W cm^{-2} (2), 0.86 W cm^{-2} (3), 8.8 W cm^{-2} (4), and 15 W cm^{-2} (5), and also of pulsed $\lambda = 248$ nm radiation of energy densities 50 mJ cm^{-2} (6) and 300 mJ cm^{-2} (7).

part of the core as a result of pulsed photoexcitation. However, simple estimates show that at the intensities employed by us the heating of a fibre is slight. For example, in the case of cw irradiation (this follows from the solution of the steady-state heat conduction equation) the temperature of a fibre core increases, compared with the temperature of the ambient medium, by

$$\Delta T \approx \frac{\alpha I(1-\gamma)r^2}{2\lambda_0} \ln\left(\frac{R}{r}\right), \quad (2)$$

where α is the absorption coefficient of the core at the excitation wavelength; I is the radiation intensity; γ is the luminescence energy yield; λ_0 is the thermal conductivity of silica glass; r and R are the radii of the core and cladding of a fibre, respectively. For typical values ($\alpha \approx 500\text{ cm}^{-1}$, $\gamma \approx 0.5$ [14], $\lambda_0 \approx 1.5 \times 10^{-2}\text{ W cm}^{-1}\text{ K}^{-1}$ [15], $r \approx 1.6\text{ }\mu\text{m}$, and $R \approx 62.5\text{ }\mu\text{m}$ at $I = 1\text{ W cm}^{-2}$), relationship (2) gives $\Delta T \approx 10^{-3}\text{ K}$.

Pulsed heating of the core can be considered on the assumption that during a laser pulse ($\tau \approx 20\text{ ns}$) there is no significant diffusion of heat from the core to the cladding, i.e. all the absorbed radiation (with the exception of photoluminescence) is transformed to heat the core:

$$\Delta T \approx \frac{\alpha E(1-\gamma)}{c\rho}, \quad (3)$$

where $c \approx 0.89\text{ W s g}^{-1}\text{ K}^{-1}$ and $\rho \approx 2.2\text{ g cm}^{-3}$ [15] are, respectively, the specific heat and density of silica glass; E is the energy density. It follows that, at the energy density $E \approx 50\text{ mJ cm}^{-2}$ used in our experiments, the core temperature rises by $\Delta T \approx 10\text{ K}$ during a laser pulse. Consequently, at moderate energy densities in a pulse, $E < 0.5\text{ J cm}^{-2}$, the heating of a fibre is slight and only at $E > 1\text{ J cm}^{-2}$ should one take heating into account, as shown in Ref. [16] for Bragg gratings ‘written’ by a single laser pulse.

The second and most important cause of the difference between the two types of interaction is the photoionisation of GODCs. Under cw irradiation conditions, the steady-state population of the excited states of GODCs is relatively low. For example, the fraction of the centres excited to the T_1 state by radiation of intensity $I_{244} = 1\text{ W cm}^{-2}$ is about 10^{-3} . When pulsed excitation is used, almost all the centres are excited during one laser pulse when the energy density

in the beam is at least 100 mJ cm^{-2} [9]. Therefore, the probability of cascade ionisation, for example from the T_1 state, increases considerably. In view of this, we can assume that the photoionisation of GODCs together with the ionisation-free transformation of GODCs from the triplet state represent the main channel which alters the RI of germanosilicate glass.

The degree of participation of the excited triplet state of GODCs in the mechanism of the induced RI was determined by a study of the dynamics of Δn_{ind} under singlet and triplet excitation conditions when the population of the state T_1 was the same in both cases. The ratio of the intensities of irradiation resulting in singlet (244 nm) and triplet (333–364 nm) excitation of GODCs, ensuring equality of the triplet luminescence signal I_0 , was determined. The irradiated fibre segments were of the same length ($L \approx 2\text{ mm}$). The luminescence signal was recorded from the end of an irradiated fibre waveguide at the wavelength 400 nm within a spectral band 1 nm wide. The excitation intensity was selected to be low ($I_{244} \sim 0.05\text{ W cm}^{-2}$) in order to avoid luminescence decay and photoinduced absorption in the investigated spectral range in the course of measurements. When the intensity ratio obtained in this way was converted, with the aid of known characteristics of the absorption lines [14] and of the laser line intensities, it was found that the ratio of the excitation efficiencies at the maxima of the absorption band was ~ 3300 , slightly higher than the ratio of the absorption coefficients in these bands $\alpha_{242}/\alpha_{330} \sim 1000$ [14] usually observed in bulk germanosilicate glass samples.

This comparison of the efficiencies of the photoexcitation of the triplet state enabled us to reduce the dynamics of the RI behaviour to a form convenient in comparison. The dependences of Δn_{ind} on $(N/N_0)t$ (N is the number of photons crossing a unit area of the fibre surface during the irradiation time t , whereas N_0 is the photon flux density giving rise to a control luminescence level I_0) are plotted in Fig. 4 for irradi-

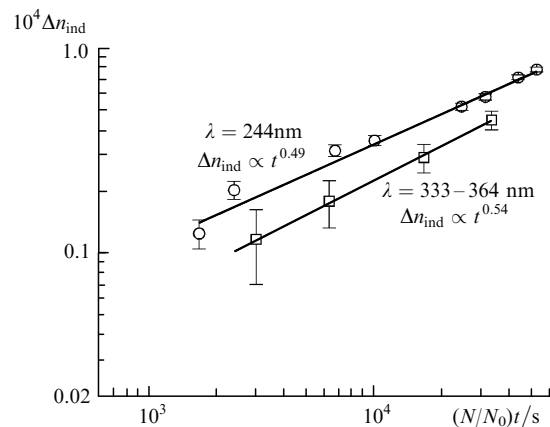


Figure 4. Dependences of Δn_{ind} on $(N/N_0)t$ for irradiation at $\lambda = 244$ and $333\text{--}364$ nm.

ation at $\lambda = 244$ and $333\text{--}364$ nm.

A comparison of these dependences led us to the conclusion that in the case of singlet photoexcitation of GODCs ($\lambda = 244$ nm) at least $(2/3)\Delta n_{\text{ind}}$ was induced with the aid of a triplet state, confirming the hypothesis put forward above. The greater efficiency of the photoinduced change in the RI in the singlet excitation case can obviously be explained by a shift of the dynamic equilibrium between

the formation and decay of the red luminescence centres, which may participate in the process of changing the refractive index. This conclusion is drawn because irradiation at $\lambda = 333\text{--}364\text{ nm}$ excites quite efficiently the absorption bands of the red-luminescence defects and, as found in our experiments, may dissociate these defects. For example, decay of the red luminescence and a reduction of the induced RI were observed in a fibre which was first irradiated at $\lambda = 244\text{ nm}$ and then at $\lambda = 333\text{--}364\text{ nm}$. However, the relationship between the concentration of the Ge-DID defects and Δn_{ind} needs to be investigated further.

4. Conclusions

We investigated and compared the dynamics of the induced RI in the core of a fibre doped with germanium and subjected to different types of pulsed and cw UV irradiation. Measurements were made with the aid of a fibre Mach–Zehnder interferometer, based on long-period photoinduced RI gratings. The induced RI is described, in a wide range of doses, by a power law ($\Delta n_{\text{ind}} \propto D^b$) and the power exponent depends on the irradiation parameters. A comparative analysis of the RI dynamics in the case of singlet and triplet excitation of GODCs showed that, in the course of low-intensity cw UV irradiation, dissociation of GODCs from the excited triplet state T_1 is the dominant mechanism in the process of inducing the RI changes.

References

1. Kashyap R *Opt. Fiber Technol.* **1** 17 (1994)
2. Hand D P, Russell P St J *Opt. Lett.* **15** 102 (1990)
3. Sceats M G, Atkins G R, Poole S B *Annu. Rev. Mater. Sci.* **23** 381 (1993)
4. Poumellec B, Guenot P, Riant I, Sansonetti P, Niay P, Bernage P, Bayon J F *Opt. Mater.* **4** 441 (1995)
5. Dianov E M, Starodubov D S, Frolov A A *Electron. Lett.* **32** 246 (1996)
6. Starodubov D S, Dianov E M, Vasiliev S A, Frolov A A, Medvedkov O I *Proc. SPIE Int. Soc. Opt. Eng.* **2998** 111 (1997)
7. Dianov E M, Starodubov D S, Vasiliev S A, Frolov A A, Medvedkov O I *Proc. SPIE Int. Soc. Opt. Eng.* **2998** 154 (1997)
8. Sulimov V B, Sokolov V O, Dianov E M, Poumellec B *Kvantovaya Elektron. (Moscow)* **23** 1013 (1996) [*Quantum Electron.* **26** 988 (1996)]
9. Bagratashvili V N, Tsypina S I, Chernov P V, Rybaltovskii A O, Zavorotny Yu S, Alimpiev S S, Simanovskii Ya O, Liang Dong, Russell P St J *Appl. Phys. Lett.* **68** 1616 (1996)
10. Dianov E M, Vasiliev S A, Kurkov A S, Medvedkov O I, Protopopov V N *Proceedings of the Twenty-Second European Conference on Optical Communication (ECOC'96), Oslo, 1996* Vol. 1, p. 65
11. Fonjallaz P Y, Limberger H G, Salathe R P, Cochet F, Leuenberger B *Opt. Lett.* **20** 1346 (1995)
12. Patrick H, Gilbert S L *Opt. Lett.* **18** 1484 (1993)
13. Williams G M, Putnam M A, Tsai T E, Askins C G, Friebele E J *OSA Tech. Digest Ser.* **22** 82 (1995)
14. Neustruev V B *J. Phys. Condens. Matter* **6** 6901 (1994)
15. Leko V K, Mazurin O V *Svoïstva Kvantsevoogo Stekla* (Properties of Quartz Glass) (Leningrad: Nauka, 1985) p. 166
16. Archambault J-L, Reekie L, Russell P St J *Electron. Lett.* **29** 453 (1993)